Scientific original paper

Informacije MIDEM
Journal of Microelectronics,
Electronic Components and Materials
Vol. 42, No. 3 (2012), 192 – 196

Electrical excitation and mechanical vibration of a piezoelectric cube

Oumar Diallo[1], E. Le Clezio[2], M. Lethiecq[1], G. Feuillard[1]

[1] Laboratoire GREMAN UMR CNRS 7347. École Nationale d'Ingénieurs du Val de Loire, Université François Rabelais de Tours, Rue de la Chocolaterie BP 3410 41034 BLOIS, CEDEX, France
[2] Institut d'Electronique du Sud UMR CNRS 5214 IES - MIRA case 082, Université Montpellier 2 Place Eugène Bataillon, 34095 MONTPELLIER CEDEX 5, France

Abstract: This work deals with the electromechanical power conversion in piezoelectric materials. In this study we will use the reverse piezoelectric effect to determine the tensorial properties of piezoelectric ceramics. The eigen vibration modes of a piezoelectric cube are modelled and characterized using resonant ultrasound spectroscopy. This method, which examines the vibration modes of a piezoelectric cube, relates mechanical resonances that can be measured by Laser interferometry to electromechanical properties. The direct problem is first solved; the resonance modes of a piezoelectric cube are modelled and mechanical displacements are calculated as functions of frequency and boundary conditions. Because the geometry of the sample is fixed, the vibrations depend only on the material properties and the electrical excitation. The displacement response of a PMN-34.5PT piezoelectric ceramic cube is investigated using a coherent optical detection. According to properties determined by electrical impedance measurements, the cube presents a first resonance around 125 kHz. Results on the amplitude of the detected velocities versus the frequency of the input excitation voltage are reported and compared to theoretical predictions. This validates the electrical modelling of the cube vibrations.

Key words: Vibration-Piezoelectricity-Spectroscopy-Eigen-frequency-Materials

Električno vzbujanje in mehanske vibracije piezoelektrične kocke

Povzetek: Delo obravnava elektrokemijsko pretvorbo energije v piezoelektričnih materialih. Za določevanje tenzijskih lastnosti piezoelektričnih keramik je uporabljen obraten piezoelektričen efekt. Načini eigenovih vibracij piezoelektrične kocke so modelirani in karakterizirani z resonančno ultrazvočno spektroskopijo. Ta metoda preko merljive mehanične resonacije z lasersko interferometrijo ugotavlja elektromehanske lastnosti. Modelirani so resonančni načini piezoelektrične kocke. Mehanični premiki so računani kot funkcija frekvence in robnih pogojev. Zaradi fiksne geometrije vzorca so vibracije odvisne le od lastnosti materiala in električne vzbujenosti. Odziv premika pmn-34.5pt piezoelektrične keramične kocke je raziskan s pomočjo koherentne optične detekcije. Prva resonančna frekvenca kocke 125 kHz je določena s pomočjo impedančnih meritev lastnosti kocke. Rezultati amplitude detektiranih hitrosti glede na frekvenco vzbujevalne napetosti so predstavljeni in primerjani s teoretičnimi ocenami, kar potrjuje električen model vibracij kocke.

Ključne besede: vibracije, piezoelektričen efekt, spektroskopija, eigen, frekvenca, materiali

** Corresponding Author's e-mail: oumar.diallo@univ-tours.fr*

1. Introduction

Several models of one-dimensional vibrations of a piezoelectric sample can be found in the literature, such as Mason's [1] and KLM [2] which can predict the electromechanical behaviour of a piezoelectric material. However, these methods are not applicable for a 3D specimen such as a cube. Until now, conventional techniques use several samples for parameter identifications [3]. Recently, Delaunay *et al.* proposed an ultrasonic characterization method allowing the determination of these properties using a single sample. This method, referred to as Resonant Ultrasound Spectroscopy [4], examines the vibration modes of a piezoelectric cube and relates mechanical resonances measured by Laser interferometry to electromechanical properties. This method is here modified to obtain the electromechanical properties taking into account

the boundary conditions. First the eigenfrequencies of a piezoelectric cube with two electrodes are calculated and compared to the eigenfrequencies of the same piezoelectric cube with only one electrode and of the sample with no electrode. Then, the velocity spectra are calculated and compared to experimental results.

2. Lagrangian minimization

From classical mechanics the general form of a Lagrangian L is expressed as:

$$L = \iiint_V (E_C - E_{def} - E_p - E_e)dV \tag{1}$$

where E_c is the kinetic energy, Edef is the deformation energy, Ep is the potential energy and Ee is the electrostatic energy.

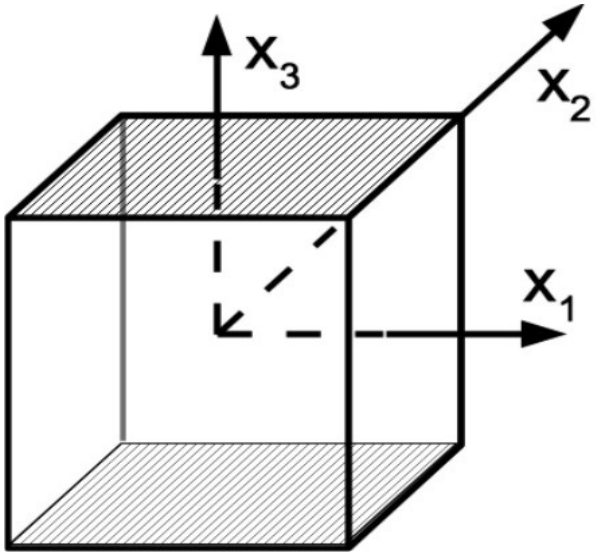

Figure 1: Piezoelectric parallelepiped of PMN-34.5PT with dimensions A,B and C poled along x_3

We consider a piezoelectric parallelepiped with dimension A, B and C (figure1). If we suppose that the origin of the axes is at the center of the cube, L_1=A/2, L_2=B/2 and L_3=C/2 where A,B and C are the edges of the cube. There are two electrodes on the planes x_3=L_3 and x_3=-L_3. The general Lagrangian can be expressed as [5 & 6]:

$$\begin{aligned} L = & \iiint_V \frac{1}{2}\left(u_{i,j} C^E_{ijkl} u_{k,l} - \rho\omega^2 u_i u_i\right) dV \\ & + \iiint_V \frac{1}{2}\left(2\phi_{,m} e_{mkl} u_{k,l} - \phi_{,m}\varepsilon^S_{mn}\phi_{,n}\right)dV \\ & - \sum_{s=1}^{2} \iint_S N_m \phi\left(e_{mkl} u_{kl} - \varepsilon^S_{mn}\phi_{,n}\right)dS, \end{aligned} \tag{2}$$

where ρ and components C^E_{ijkl}, e_{mkl}, and ε^S_{mn} are respectively, the density, the elastic stiffness tensor measured at constant electrical field, the piezoelectric tensor and the dielectric tensor measured at constant strain of the material. The summation on indices runs from 1 to 3, corresponding to the three directions in the coordinate space. u is the displacement field and ϕ is the potential.

To minimize the Lagrangian (and hence find the equilibrium configuration of the system), the Rayleigh-Ritz method is used. In accordance with this method the displacement and potential may be expressed as a linear combination of the trial functions:

$$u_i = \sum_{p=1}^{N} a_p \psi_p, \tag{3}$$

$$\phi = \sum_{r=1}^{M} b_r \varphi_r. \tag{4}$$

The $(\psi_p)_{p...1}$ and $(\varphi_r)_{r...M}$ functions are chosen to be orthonormal.

If these relations are injected in equation (2), the Lagrangian becomes:

$$L = \frac{1}{2}\left[\sum_p \sum_{p'} a_p a'_{p'}\left(\Gamma'_{pp'} - \rho\omega^2\delta'_{pp'}\right)\right] + \left[\sum_p \sum_r a_p b_r\left(\Omega_{pr} - A_{pr}\right)\right] - \frac{1}{2}\left[\sum_r \sum_{r'} b_r b'_{r'}\left(\Lambda'_{rr'} - 2B'_{rr'}\right)\right] \tag{5}$$

Where

$$\begin{aligned} \Gamma_{pp'} &= \iiint \psi_{pi,j} C^E_{ijkl} \psi_{p'k,l}\, dV \\ \Omega_{pr} &= \iiint \varphi_{r,m} e_{mkl} \psi_{pk,l}\, dV, \\ \Lambda'_{rr'} &= \iiint \varphi_{r,m} \varepsilon^S_{mn} \varphi_{r',n}\, dV, \\ A_{pr} &= \sum_{S=1}^{2} \iint \varphi_r N_m e_{mkl} \psi_{pk,l}\, dS, \\ B'_{rr'} &= \sum_{S=1}^{2} \iint \varphi_r N_m \varepsilon^S_{mn} \varphi_{r',n}\, dS \end{aligned} \tag{6}$$

with

$$\psi_{pi,j} = \frac{1}{2}\left(\frac{\partial\psi_{pi}}{\partial x_j} + \frac{\partial\psi_{pj}}{\partial x_i}\right) \quad and \quad \varphi_{r,m} = \frac{\partial\varphi_r}{\partial x_m}. \tag{7}$$

Γ, Ω and Λ are respectively elastic, piezoelectric and dielectric interaction matrices. A_{pr} and $B_{rr'}$ are the contributions of the work of the electrostatic forces. Coefficients ap and br are obtained by calculating the stationary points of the Lagrangian (*i.e.* $\partial L = 0$). This yields the following eigenvalue system:

$$(\Gamma + (\Omega - A)(\Lambda - 2B)^{-1}(\Omega - A)^t)a = \rho\omega^2 a,$$
$$b = (\Lambda - 2B)^{-1}(\Omega - A)^t a. \quad (8)$$

The eigenvectors of this equation system give us the coefficients of the expansion of the actual displacement and the electrical functions in terms of the basis functions. The eigenvalues correspond to the actual resonance frequencies.

3. Eigen vibration modes of a piezoelectric cube

Choice of the basis functions

In 1971 H. Demarest introduced the use of Legendre polynomial to determine the elastic constants of a solid [7]. A few years later I. Ohno extended this use to the study of free vibrations of a crystal [6]. Recently, Delaunay *et al.* proposed basis functions for a piezoelectric specimen with an electrode on one face of a parallelepipedic crystal [4]. In this study, two electrodes are placed on the cube: one on the face x_3=-L_3 and one on the face x_3=L_3. These faces are normal to the poling direction and the chosen basis function must verify:

$$\delta_{pp'} = \begin{cases} 1 & if\ p = p' \\ 0 & otherwise \end{cases} \quad (9)$$

The displacement basis functions defined by Demarest are unchanged. These functions were verified by Ohno and Delaunay *et al.*. The electrical function is here modified to simulate the short-circuit boundary conditions, *i.e.* the potential on face x3=-L3 must be equal to the potential on face x3=L3. We suppose that the potential on the electrodes null in order to set to zero the A_{pr} and $B_{rr'}$ matrices and thus minimize the computation time. The chosen basis functions of the displacements and electrical potential are respectively:

$$\psi_p = \frac{1}{\sqrt{L_1 L_2 L_3}} P_\lambda\left(\frac{x_1}{L_1}\right) P_\mu\left(\frac{x_2}{L_2}\right) P_\nu\left(\frac{x_3}{L_3}\right) e_i, \quad (10)$$

$$\varphi_r = \frac{1}{\sqrt{L_1 L_2 L_3}} P_\xi\left(\frac{x_1}{L_1}\right) P_\zeta\left(\frac{x_2}{L_2}\right) f_\eta\left(\frac{x_3}{L_3}\right) \quad (11)$$

With $f_\eta\left(\frac{x_3}{L_3}\right) = sin\left((\eta+1)\left(1+\frac{x_3}{L_3}\right)\right) P_\eta\left(\frac{x_3}{L_3}\right)$ where the p^{th} and r^{th} basic functions ψ_p and φ_r are defined by the triplets, ($\lambda w,\mu,\nu$) and (ξ,ς,η), respectively. $P_a(x)$ is the normalized Legendre function of order α and e_i is the unit displacement vector in x_i direction, $\frac{1}{\sqrt{L_1 L_2 L_3}}$ is a normalization term [4, 6, 7].

Simulation Results

Table 1 shows the resonance frequencies of a PMN-34.5PT cube calculated using this theory and its comparison with Demarest's and Delaunay's theories. The elastic, piezoelectric and dielectric constants were taken from [4]. They are C_{11}=174.7, C_{12}=116.6, C_{13}=119.3, C_{33}=154.8, C_{44}=26.7, C_{66}=29 in GPa; e_{15}=17.1, e_{31}=-6.4, e_{33}=27.3 in C/m²; ε_1=21.0105, ε_3=25.0125 in pF/m.

Table1: Resonant for a PMN 34,5PT with Delaunay coef. (in Hz)

Demarest Basis Functions Order=7	Delaunay Basis Functions Order=7	Our Basis Functions Order=5	Error (1&2)	Error (1&3)
82966	86778	87007	-4.59%	-4.87%
89241	90037	89145	-0.89%	0.11%
109147	107743	104243	1.29%	4.49%
118057	117423	113436	0.54%	3.91%
119489	121678	116894	-1.83%	2.17%
126991	122818	120120	3.29%	5.41%
129809	134243	122440	-3.42%	5.68%
134243	137977	124276	-2.78%	7.42%
139246	139264	133209	-0.01%	4.34%
142298	143193	134259	-0.63%	5.65%
145232	147165	145273	-1.33%	-0.03%
153129	153961	154155	-0.54%	-0.67%
160024	156405	156825	2.26%	2.00%
161706	163513	160742	-1.12%	0.60%

Table 1 presents the comparison between the resonant frequencies computed with the basis functions corresponding to different boundary conditions showing that the presence of the electrodes can greatly affect the resonances. Note that the volume of the electrodes has been neglected in theoretical studies. The modes with maximum displacements along the x_3 axis are the most sensitive to the presence of electrodes. The maximum difference between Demarest and Delaunay cases is 4.59% and the maximum difference between Demarest and our case is 7.42%. Increasing the degree of the approximate polynomial functions does not reduce the discrepancy in the prediction of resonant frequencies between Demarest basis function and our basis function. They are due to the new boundary conditions (short circuit electrodes). The order of the basis functions in our case is lower than in Demarest and Delaunay's cases; the convergence is improved and the computing time is around 2.2 seconds against 22.4 seconds for Demarest.

4. Experimental results

Experimental set-up

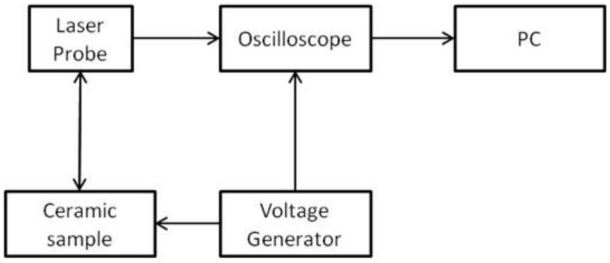

Figure 2: Experimental set-up

The experimental set-up is presented on figure 2. It allows the measurement of vibration velocities versus frequency. The electrical excitation is delivered by a voltage generator. It has a very large bandwidth and the delivered electrical power is adjustable. The sample is set on a plastic holder and the electrical contact is ensured by a metallic strip fixed on a spring so that free mechanical boundary conditions at the surfaces of the cube are fulfilled. Velocities at the surface of the sample are measured by means of a Laser vibrometer (Polytech OFV-505) that allows the detection of the resonance frequencies and the identification of the associated mode shapes. The interferometer is positioned at 50 cm from the sample. The velocity decoder sensitivity is respectively 5 mm/s/V and 25 mm/s/V, depending on the cut-off frequency, respectively 250 kHz and 1.5 MHz. The measured signals are sent to a computer via a digital oscilloscope.

Results and discussions

The resonance spectrum of the PMN-34.5PT (10mm×10mm×10mm) sample was measured by the described above experimental set-up.

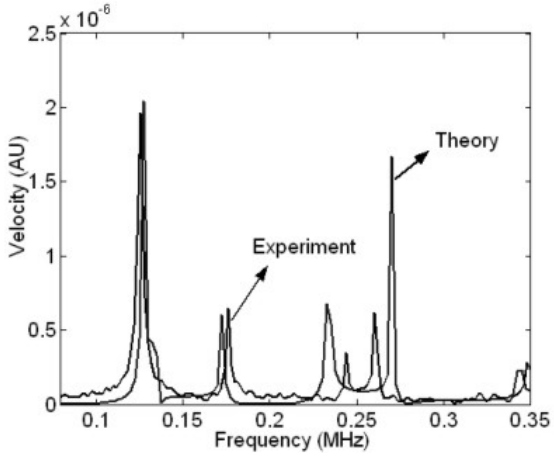

Figure 3: Comparison between the theoretical and experimental velocity spectra of the PMN-34.5PT cube (at the center of the face $x_{3=L3)}$

Experimental and theoretical results are compared in Figure 3. The theoretical velocity is computed using the eigen frequencies and the expression of the displacement, the velocity being the time derivative of the displacement. In the frequency domain, this implies: $v = j\omega u$.

For the first two resonances, agreement is satisfactory. The discrepancies between measurements and predictions for the two other peaks could be due to the lack of precision in the functional properties used for the theoretical modeling. A sensitivity study of the resonance location to input parameters has shown that these two peaks were very sensitive to C_{13} and C_{33}. Further studies will deal with the application of the model to material characterization.

5. Conclusion

This paper studied the natural frequencies of a piezoelectric ceramic. A numerical method is developed to predict the resonance spectrum of the PMN-34.5PT cube and a comparison with the experimental spectrum shows that all the eigenfrequencies are not piezoelectrically coupled. In future work, the inverse problem will be solved for this and other piezoelectric ceramics in order to extract the functional properties of piezoelectric ceramics from their resonant spectra.

Appendix

A. Description of interaction matrices: elastic, Γ, piezoelectric, Ω, and dielectric Λ

Table2: Matrix of elastic interaction: Γ,

i, j	Γ'_{pp}
1,1	$C_{11}^{E}G_1 + C_{66}^{E}G_2 + C_{55}^{E}G_3 + C_{56}^{E}G_4 + C_{56}^{E}G_5 + C_{15}^{E}G_6 + C_{15}^{E}G_7 + C_{16}^{E}G_8 + C_{16}^{E}G_9$
2,2	$C_{66}^{E}G_1 + C_{22}^{E}G_2 + C_{44}^{E}G_3 + C_{24}^{E}G_4 + C_{24}^{E}G_5 + C_{46}^{E}G_6 + C_{46}^{E}G_7 + C_{26}^{E}G_8 + C_{26}^{E}G_9$
3,3	$C_{55}^{E}G_1 + C_{44}^{E}G_2 + C_{33}^{E}G_3 + C_{14}^{E}G_4 + C_{14}^{E}G_5 + C_{35}^{E}G_6 + C_{35}^{E}G_7 + C_{36}^{E}G_8 + C_{36}^{E}G_9$
2,3	$C_{56}^{E}G_1 + C_{24}^{E}G_2 + C_{34}^{E}G_3 + C_{44}^{E}G_4 + C_{23}^{E}G_5 + C_{36}^{E}G_6 + C_{45}^{E}G_7 + C_{25}^{E}G_8 + C_{46}^{E}G_9$
3,1	$C_{15}^{E}G_1 + C_{46}^{E}G_2 + C_{35}^{E}G_3 + C_{36}^{E}G_4 + C_{45}^{E}G_5 + C_{55}^{E}G_6 + C_{13}^{E}G_7 + C_{14}^{E}G_8 + C_{56}^{E}G_9$
1,2	$C_{16}^{E}G_1 + C_{26}^{E}G_2 + C_{45}^{E}G_3 + C_{25}^{E}G_4 + C_{46}^{E}G_5 + C_{14}^{E}G_6 + C_{56}^{E}G_7 + C_{66}^{E}G_8 + C_{12}^{E}G_9$

Table3: Matrix of piezoelectric interaction: Ω

i	Ω_{pr}
1	$e_{11}G_1 + e_{26}G_2 + e_{35}G_3 + e_{25}G_4 + e_{36}G_5 + e_{31}G_6 + e_{15}G_7 + e_{16}G_8 + e_{21}G_9$
2	$e_{16}G_1 + e_{22}G_2 + e_{34}G_3 + e_{24}G_4 + e_{32}G_5 + e_{36}G_6 + e_{14}G_7 + e_{12}G_8 + e_{26}G_9$
3	$e_{15}G_1 + e_{24}G_2 + e_{33}G_3 + e_{23}G_4 + e_{34}G_5 + e_{35}G_6 + e_{13}G_7 + e_{14}G_8 + e_{25}G_9$

Table4: Matrix of dielectric interaction: Λ

Λ'_{rr}
$\varepsilon_{11}^{S}G_1 + \varepsilon_{22}^{S}G_2 + \varepsilon_{33}^{S}G_3 + \varepsilon_{23}^{S}G_4 + \varepsilon_{32}^{S}G_5 + \varepsilon_{13}^{S}G_6 + \varepsilon_{31}^{S}G_7 + \varepsilon_{12}^{S}G_8 + \varepsilon_{21}^{S}G_9$

B. presentation of the f_h functions:

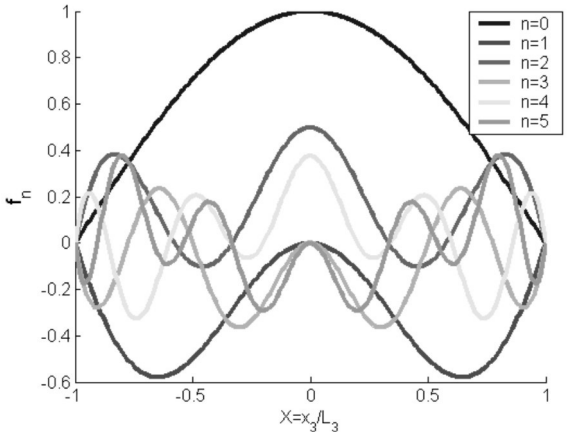

References

1. W. P. Mason, N. J. Princeton & V. Nostrand, Eds. Physical Review (2nd Edition, Vol. **72**) (1948)
2. R. Krimholtz, D. A. Leedom, & G. L. Matthaei, *Electronic Letters*, ***6***, 398–399 (1970).
3. ANSI/IEEE Standard 176-1987 on piezoelectricity, IEEE Trans. Ultrason., Ferroelect., Freq. Contr. **43**, 717 (1996).
4. T. Delaunay et al., IEEE Trans. on UFFC control **55**, 476 (2008).
5. R. Holland et al, IEEE Trans. on Sonics and Ultrasonics, 119 (1968)
6. I. Ohno, J. Phys. Earth, **24**,355(1976)
7. H. Demarest, J. Acous. Soc. Am., **49**, 768 (197

Arrived: 11. 09. 2012
Accepted: 13. 11. 2012